Appendix Figures and Table

SARS-CoV-2 spike protein stimulates MAP4K3/GLK-induced ACE2 stabilization in COVID-19

Huai-Chia Chuang, Chia-Hsin Hsueh, Pu-Ming Hsu, Rou-Huei Huang, Ching-Yi Tsai, Nai-Hsiang Chung, Yen-Hung Chow, Tse-Hua Tan

Table of contents

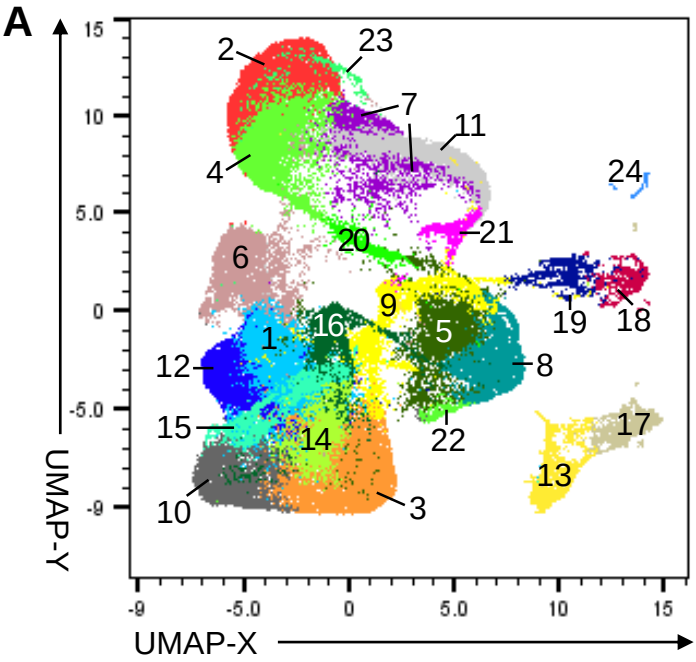

Cluster classification:

Macrophages (CD68$^+$): 1, 3, 6, 10, 12, 14, 16
Neutrophils (FCGR3B$^+$): 15
T cells (CD3D$^+$): 5, 8
B cells (MS4A1$^+$): 9
Plasma cells (IGHG4$^+$): 18,19
NK cells (KLRD1$^+$): 22
Dendritic cells (CD1C$^+$, CLEC9A$^+$): 2, 7
Ciliated epithelial cells (KRT18$^+$, TPPP3$^+$): 13
Epithelial cells (KRT18$^+$): 17

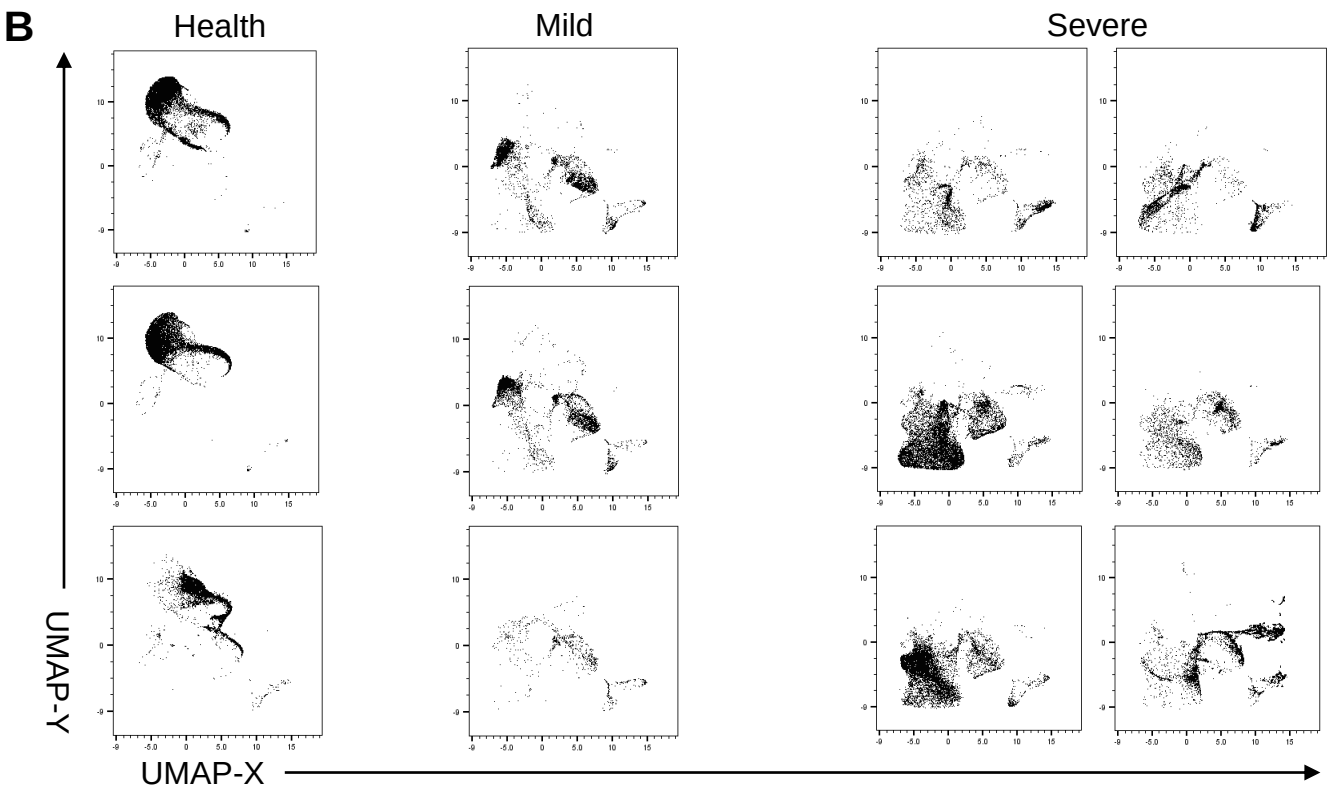

Appendix Figure S1. Distribution and classification of individual cell types within human bronchoalveolar lavage fluid (BALF) cells. (**A**) Distribution and classification of BALF cells from all 12 individuals of Cohort #1 (Reference #9). Data are shown in UMAP. (**B**) Individual distributions of BALF cells from 3 healthy controls (HC), 3 mild COVID-19 patients, and 6 severe COVID-19 patients. Cell populations were defined as described (Liao *et al*., 2020).

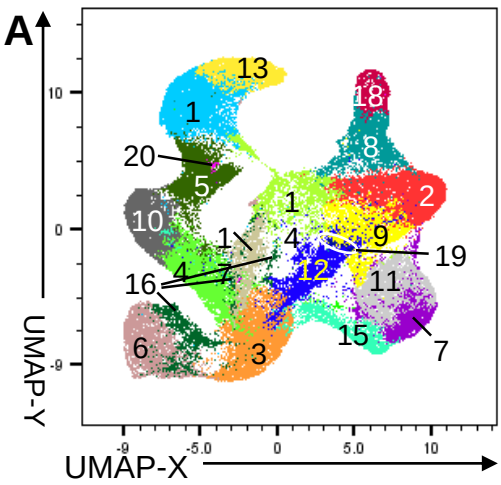

Cluster classification:

Macrophages (CD68$^+$): 5, 18
Neutrophils (FCGR3B$^+$): 13
T cells (CD3D$^+$): 6, 16
B cells (MS4A1$^+$): 17
NK cells (KLRD1$^+$): 6
Dendritic cells
(CD1C$^+$, CLEC9A$^+$): 1
Ciliated epithelial cells
(KRT18$^+$, TPPP3$^+$): 7, 9, 11
Epithelial cells (KRT18$^+$): 2, 8

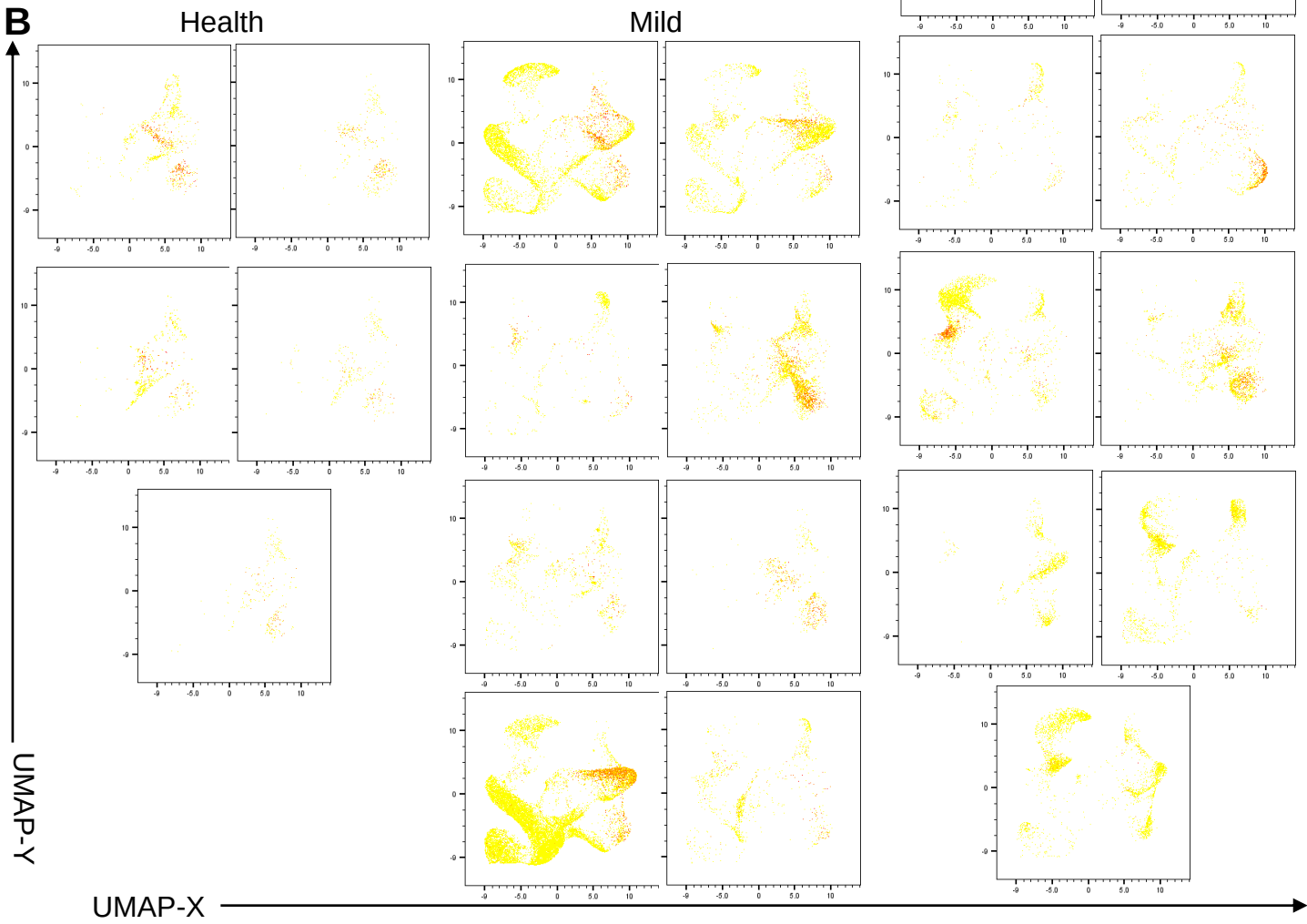

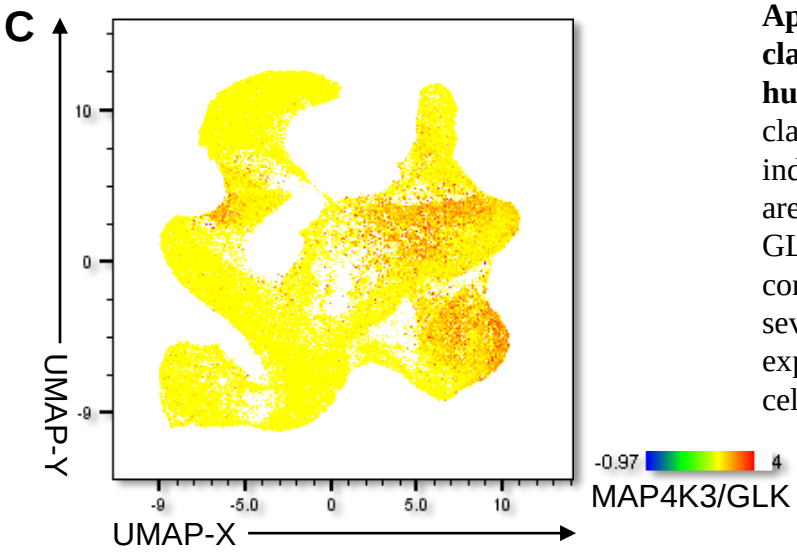

Appendix Figure S2. Distribution and classification of individual cell types within human nasal swab cells. (**A**) Distribution and classification of nasal swab cells from all 24 individuals of Cohort #2 (Chua *et al*., 2020). Data are shown in UMAP. (**B**) Individual distributions of GLK-positive nasal swab cells from 5 healthy controls (HC), 8 mild COVID-19 patients, and 11 severe COVID-19 patients. (**C**) Single-cell gene expression of MAP4K3 (GLK) in all individual cells is shown in color scale.

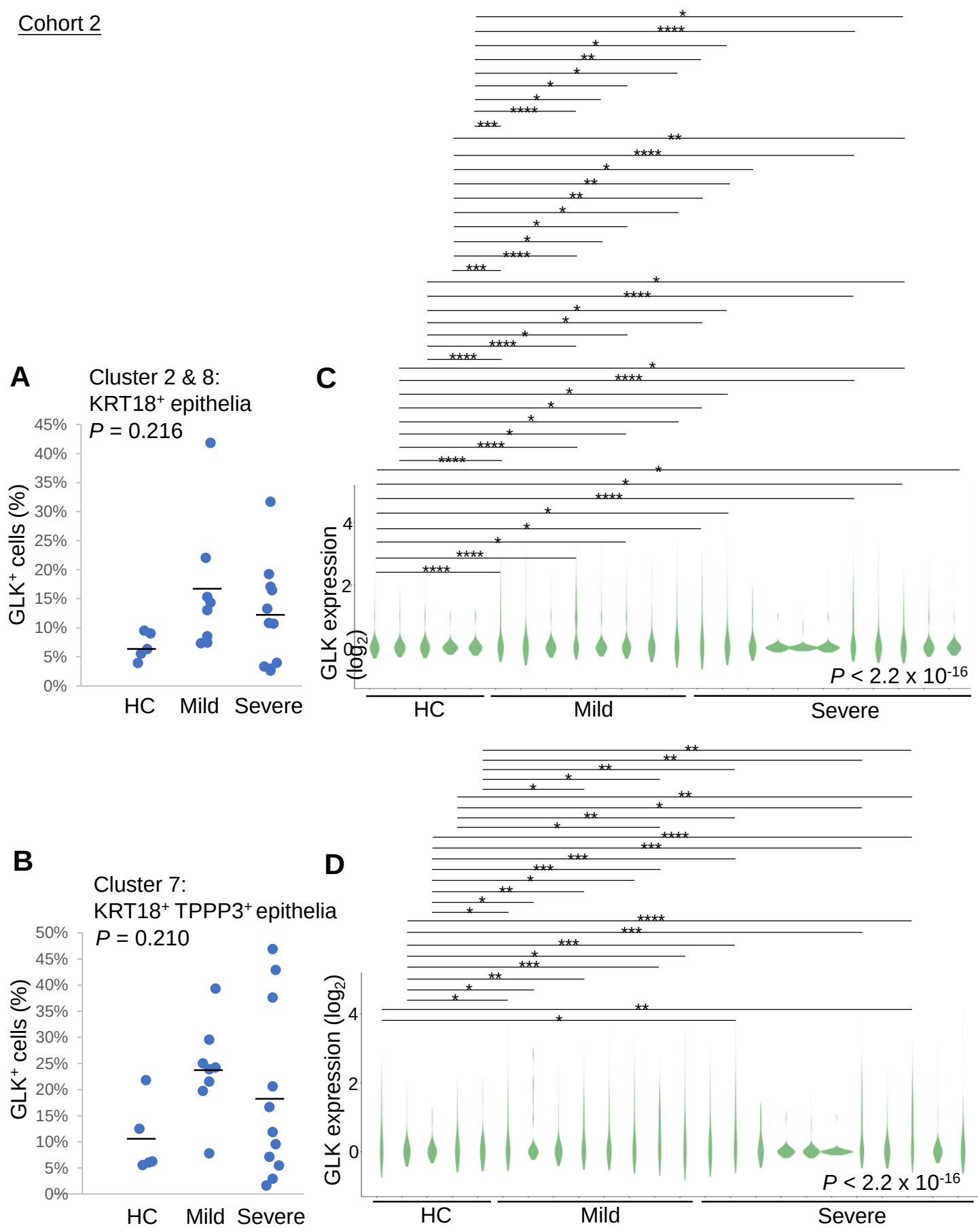

Appendix Figure S3. GLK mRNA levels are increased in human nasal swab cells of COVID-19 patients. (**A** and **B**) The percentages of MAP4K3/GLK-positive KRT18$^+$ epithelial (A) or KRT18$^+$ TPPP3$^+$ ciliated cells (B) in the nasopharynx from 5 healthy controls (HC), 8 mild COVID-19 patients, and 11 severe COVID-19 patients (Cohort #2). *, *P* value < 0.05 (ANOVA test). (**C** and **D**) GLK mRNA levels in KRT18$^+$ epithelial (C) or KRT18$^+$ TPPP3$^+$ ciliated epithelial cells (D) of Cohort #2. *, *P* value < 0.05; **, *P* value < 0.01; ***, *P* value < 0.001; ****, *P* value < 0.0001 (*Kruskal-Wallis* test).

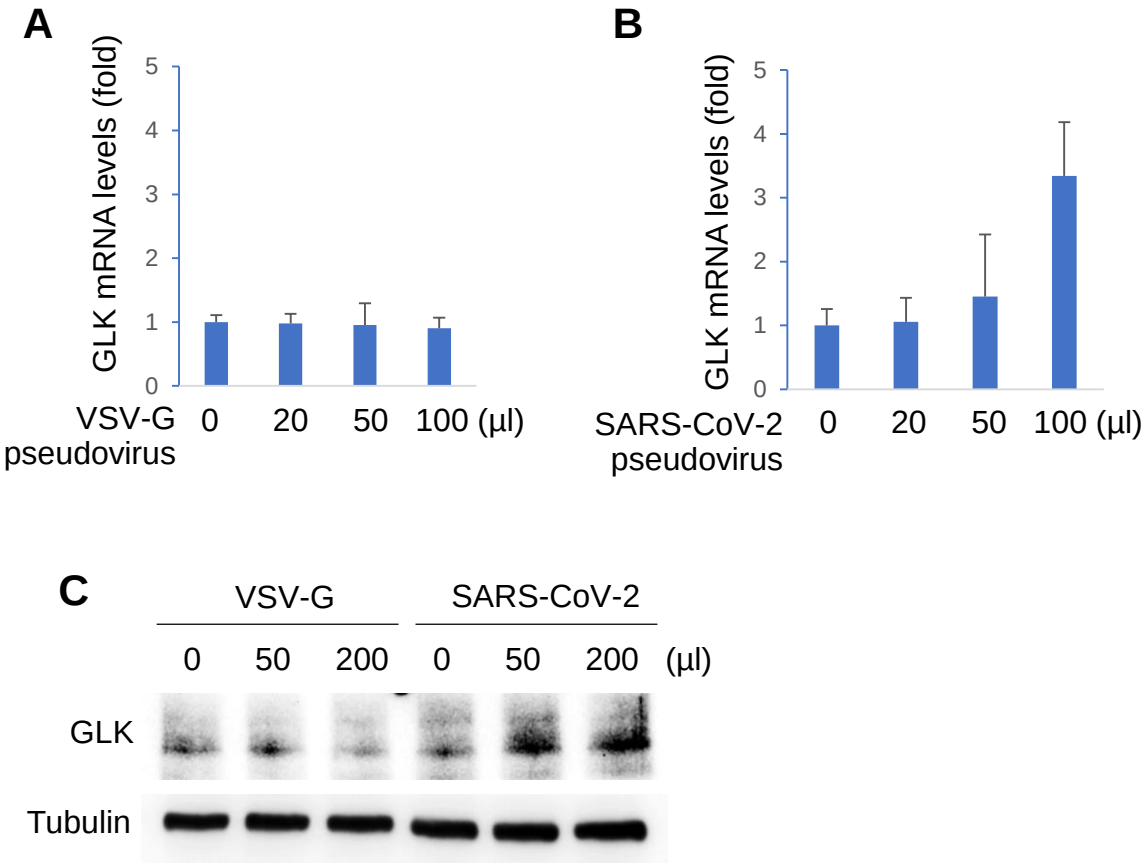

Appendix Figure S4. GLK levels are increased by SARS-CoV-2 pseudovirus. (**A** and **B**) Endogenous GLK levels were increased by SARS-CoV-2 pseudovirus infection. Real-time PCR analysis of mouse GLK mRNA levels in HCC827 lung epithelial cells either infected with VSV-G pseudotyped lentivirus (A) or SARS-CoV-2 pseudotyped lentivirus (B) for 24 h. The mRNA levels of GLK were normalized to GAPDH mRNA levels. Means ± SD are shown. Immunoblotting analysis of the endogenous GLK and tubulin proteins from the lysates of HCC827 lung epithelial cells either infected with VSV-G pseudovirus or SARS-CoV-2 pseudovirus for 24 h. Pseudovirus concentration: 1.2×10^5 copies/μl.

Cohort 3

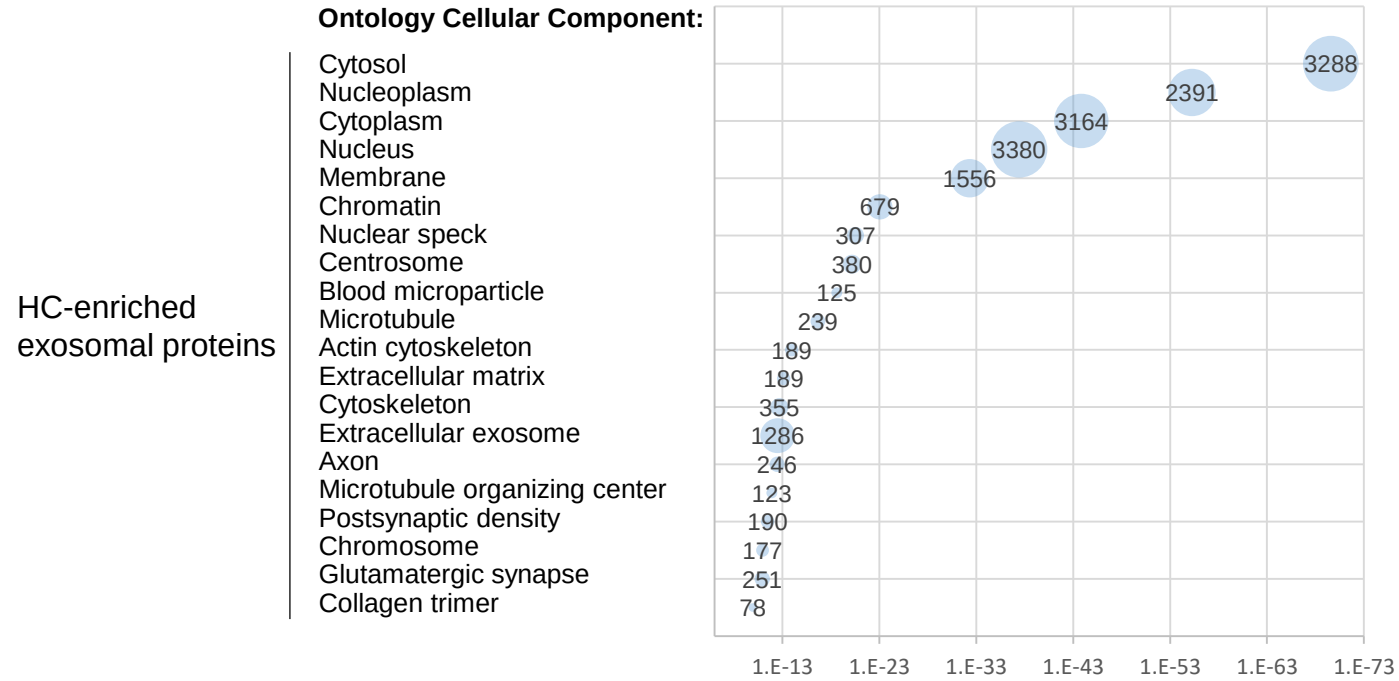

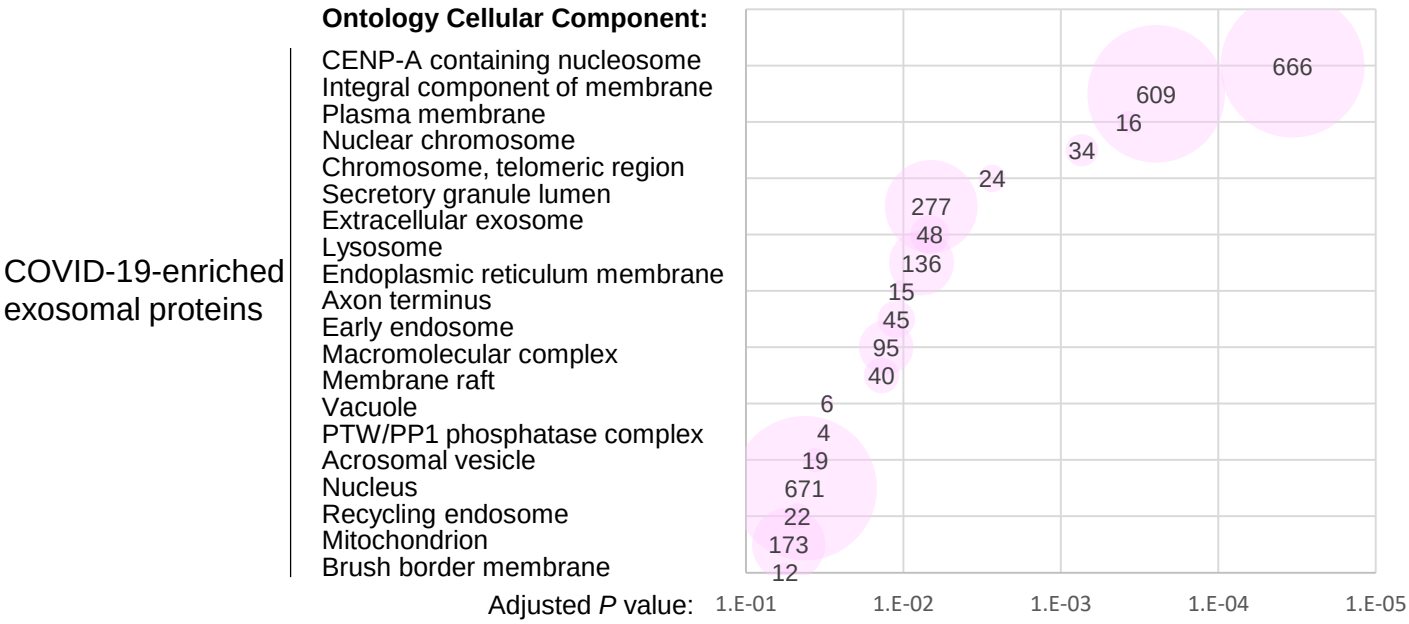

Appendix Figure S5. COVID-19-enriched exosomal proteins mainly belong to membrane proteins by Ontology Cellular Component analysis. (**A** and **B**) Ontology Cellular Component analysis of the healthy control (HC)-enriched exosomal proteins (A) and COVID-19 patient-enriched exosomal proteins (B). HC-enriched exosomal proteins were identified by mass spectrometry proteomics and then by excluding exosomal proteins identified from COVID-19 patients. COVID-19 patient-enriched exosomal proteins were identified by excluding exosomal proteins identified from HC. Cellular components belonging to different classifications are listed on the left side of the plot. Varied numbers of genes enriched in individual pathways are presented by different diameter sizes and numbers for individual dots. Adjusted *P* value is ranging from 0~1; less *P* value means greater intensiveness.
Source data are available online for this figure.

Cohort 3

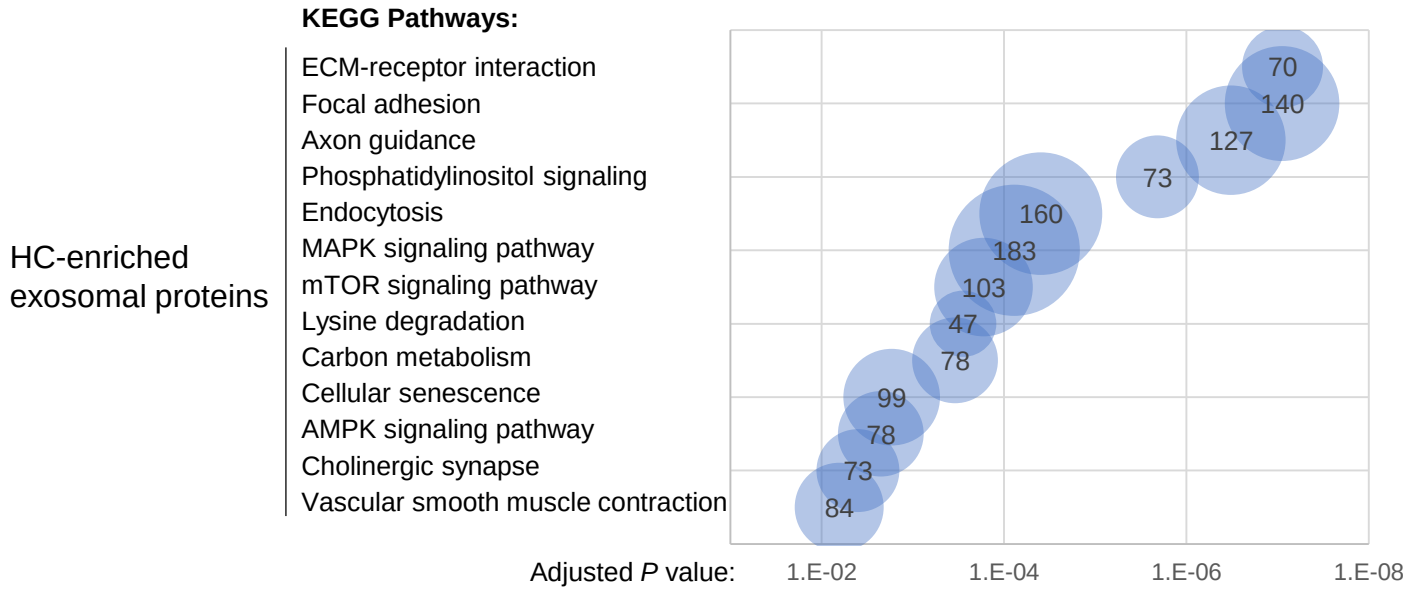

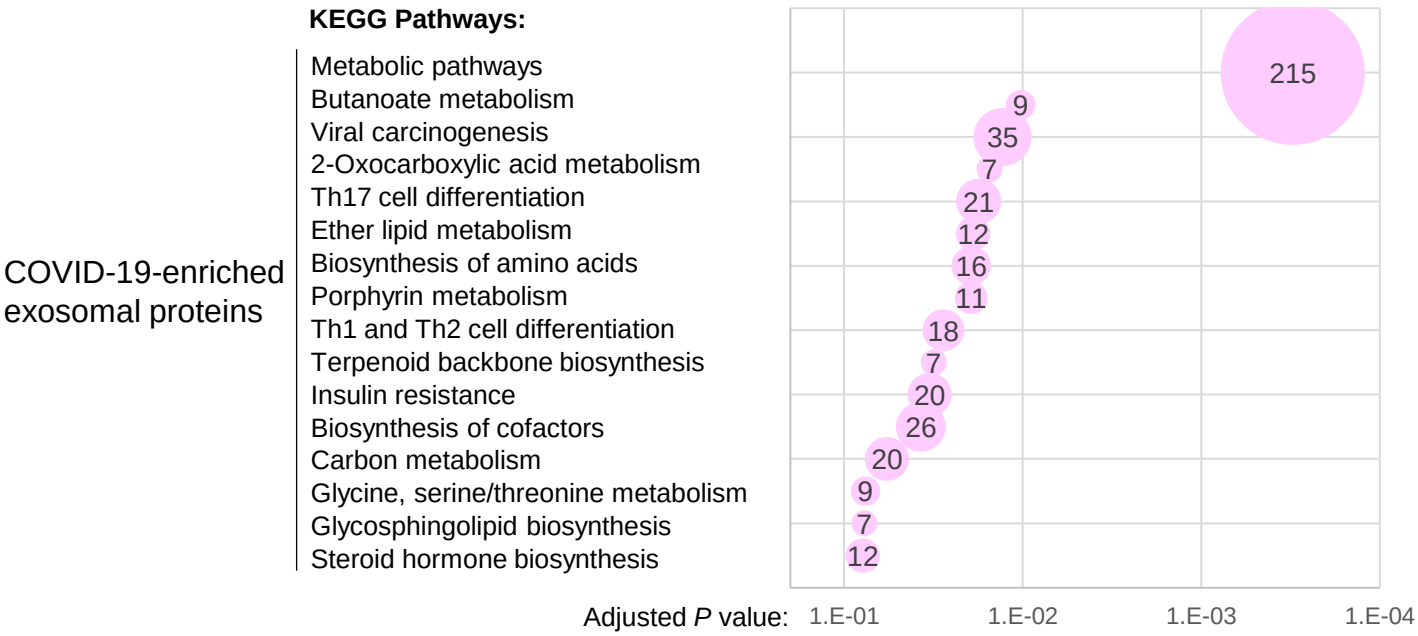

Appendix Figure S6. COVID-19 enriched exosomal proteins mainly belong to metabolic pathways by KEGG analysis. (**A** and **B**) KEGG (Kyoto Encyclopedia of Genes and Genomes) enriched pathways of the healthy control (HC)-enriched exosomal proteins (A) and COVID-19 patient-enriched exosomal proteins (B). HC-enriched exosomal proteins were identified by mass spectrometry proteomics and then by excluding exosomal proteins identified from COVID-19 patients. COVID-19 patient-enriched exosomal proteins were identified by excluding exosomal proteins identified from HC. Pathways belonging to different classifications are listed on the left side of the plot. Varied numbers of genes enriched in individual pathways are presented by different diameter sizes and numbers for individual dots. Adjusted *P* value is ranging from 0~1; less *P* value means greater intensiveness.
Source data are available online for this figure.

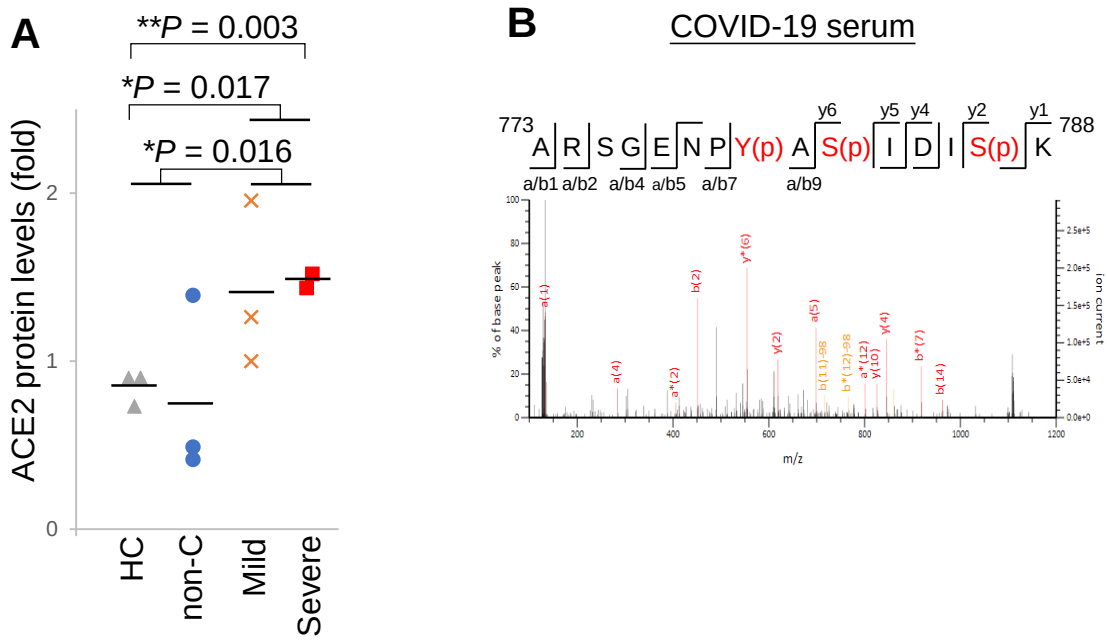

Appendix Figure S7. Phosphorylated ACE2 proteins are detected in serum samples from COVID-19 patients. (**A**) Relative levels of ACE2 proteins that were detected in serum samples from COVID-19 patients (batch 1 of Cohort #4) are calculated according to the TMTpro-labeled signals. HC, healthy controls; non-C, non-COVID-19 controls; mild, mild COVID-19 patients, severe, severe COVID-19 patients. (**B**) Mass spectrometry analysis of the ACE2 peptides containing Ser776 and Ser783 residues from COVID-19 patient sera. Phospho-Ser776, Ser783, and Tyr781 residues of ACE2 proteins detected in serum samples of COVID-19 patients (Cohort #4) are shown.

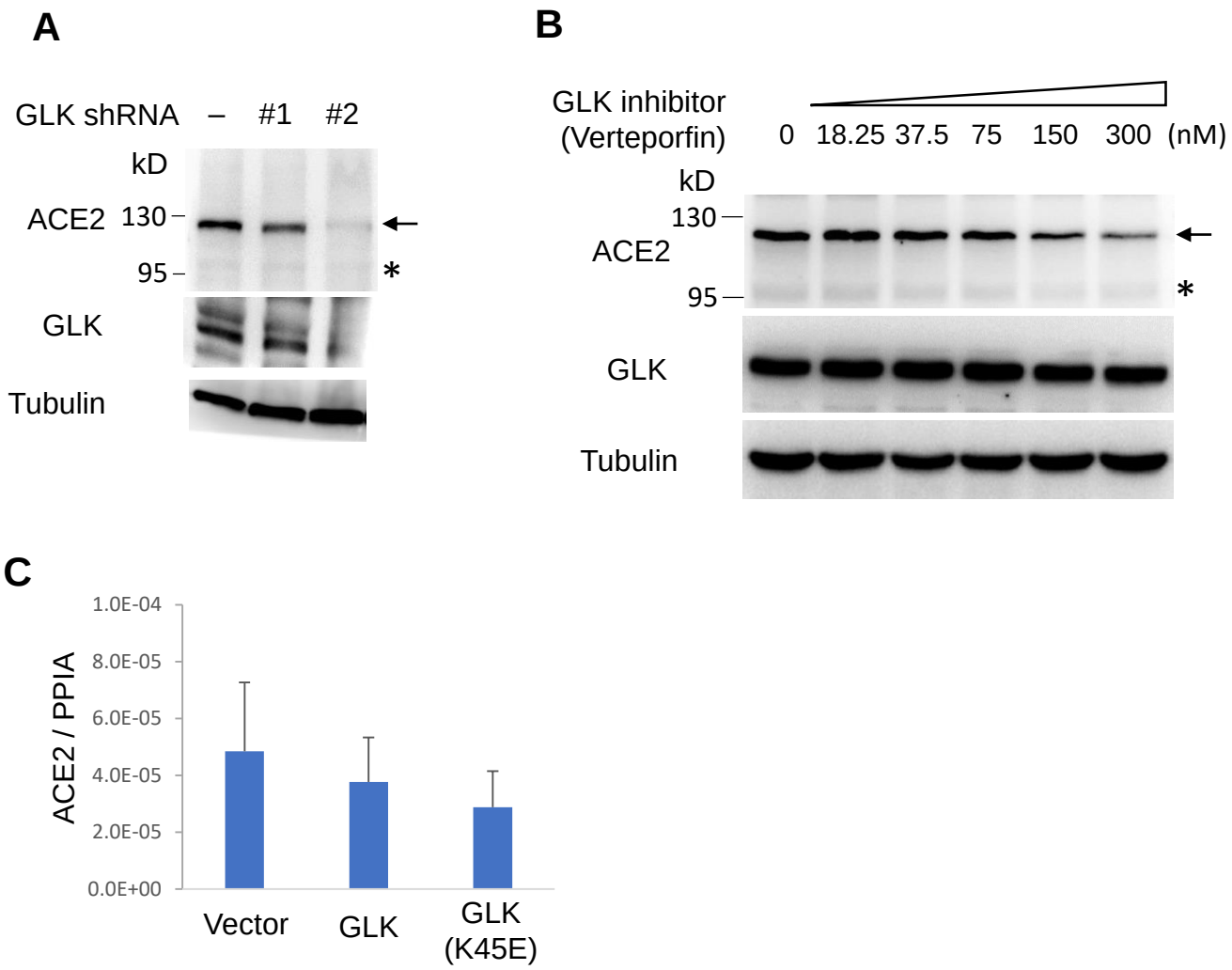

Appendix Figure S8. Endogenous ACE2 protein levels are decreased by GLK shRNA knockdown or GLK inhibitor treatment. (**A**) Immunoblotting analysis of the endogenous ACE2 and GLK proteins from the lysates of H661 lung epithelial cells transfected with GLK shRNA#1 or shRNA#2. Arrowhead denotes glycosylated ACE2 proteins; asterisk denotes unglycosylated ACE2 proteins. (**B**) Immunoblotting analysis of endogenous ACE2 and GLK proteins from the lysates of H661 lung epithelial cells treated with the GLK inhibitor verteporfin for 24 h. Arrowhead denotes glycosylated ACE2 proteins; asterisk denotes unglycosylated ACE2 proteins. (**C**) Human ACE2 mRNA levels in HCC827 lung epithelial cells transfected with vector, GLK, or GLK (K45E) kinase-dead mutant were analyzed by real-time PCR. The expression levels of ACE2 were normalized to peptidylprolyl isomerase A (PPIA) levels. Means ± SD are shown. Data shown are representative results of three independent experiments.

Appendix Table S1. Human ACE2 peptides detected in sera of COVID-19 patients of Cohort #4

Start − End	Score	Human ACE2 Peptides
2 − 26	15	M.SSSSWLLLSLVAVTAAQSTIEEQAK.T + Phospho (ST); GlyGly (K)
2 − 31	9	M.SSSSWLLLSLVAVTAAQSTIEEQAKTFLDK.F + Phospho (ST); LeuArgGlyGly (K)
2 − 31	17	M.SSSSWLLLSLVAVTAAQSTIEEQAKTFLDK.F + 5 Phospho (ST); GlyGly (K)
95 − 112	15	K.LQLQALQQNGSSVLSEDK.S + Phospho (ST); GlyGly (K)
95 − 112	17	K.LQLQALQQNGSSVLSEDK.S
113 − 131	15	K.SKRLNTILNTMSTIYSTGK.V + 4 Phospho (ST)
113 − 131	14	K.SKRLNTILNTMSTIYSTGK.V + 5 Phospho (ST); Phospho (Y); GlyGly (K); LeuArgGlyGly (K)
113 − 131	15	K.SKRLNTILNTMSTIYSTGK.V + 6 Phospho (ST); Phospho (Y); GlyGly (K); LeuArgGlyGly (K)
115 − 131	14	K.RLNTILNTMSTIYSTGK.V + Phospho (ST); GlyGly (K)
115 − 131	6	K.RLNTILNTMSTIYSTGK.V + Phospho (ST); GlyGly (K)
115 − 131	14	K.RLNTILNTMSTIYSTGK.V + Phospho (ST); GlyGly (K)
115 − 131	15	K.RLNTILNTMSTIYSTGK.V + 2 Phospho (ST); GlyGly (K)
115 − 131	15	K.RLNTILNTMSTIYSTGK.V + Phospho (ST)
116 − 131	13	R.LNTILNTMSTIYSTGK.V + Phospho (ST); GlyGly (K)
116 − 131	9	R.LNTILNTMSTIYSTGK.V + Phospho (ST); GlyGly (K)
116 − 131	14	R.LNTILNTMSTIYSTGK.V + Phospho (ST); GlyGly (K)
116 − 131	7	R.LNTILNTMSTIYSTGK.V + Phospho (ST); GlyGly (K)
116 − 131	19	R.LNTILNTMSTIYSTGK.V + Phospho (ST); GlyGly (K)
116 − 131	14	R.LNTILNTMSTIYSTGK.V + Phospho (ST); GlyGly (K)
116 − 131	11	R.LNTILNTMSTIYSTGK.V + Phospho (ST); GlyGly (K)
116 − 131	15	R.LNTILNTMSTIYSTGK.V + 2 Phospho (ST); GlyGly (K)
116 − 131	12	R.LNTILNTMSTIYSTGK.V
116 − 131	5	R.LNTILNTMSTIYSTGK.V
116 − 131	11	R.LNTILNTMSTIYSTGK.V + Phospho (ST)
170 − 187	12	R.SEVGKQLRPLYEEYVVLK.N + Phospho (ST); 2 LeuArgGlyGly (K)
205 − 219	9	R.GDYEVNGVDGYDYSR.G + Phospho (ST)
307 − 313	3	R.IFKEAEK.F + 2 GlyGly (K)
307 − 313	3	R.IFKEAEK.F + 2 GlyGly (K)
310 − 353	17	K.EAEKFFVSVGLPNMTQGFWENSMLTDPGNVQKAVCHPTAWDLGK.G + Carbamidomethyl (C); 2 Phospho (ST); GlyGly (K); LeuArgGlyGly (K)
310 − 353	14	K.EAEKFFVSVGLPNMTQGFWENSMLTDPGNVQKAVCHPTAWDLGK.G + Carbamidomethyl (C); 2 Phospho (ST); GlyGly (K); LeuArgGlyGly (K)

354 − 363	7	K.GDFRILMCTK.V + GlyGly (K)
354 − 363	5	K.GDFRILMCTK.V + GlyGly (K)
354 − 363	5	K.GDFRILMCTK.V + GlyGly (K)
354 − 363	14	K.GDFRILMCTK.V + GlyGly (K)
420 − 441	17	K.SIGLLSPDFQEDNETEINFLLK.Q + Phospho (ST); LeuArgGlyGly (K)
420 − 458	15	K.SIGLLSPDFQEDNETEINFLLKQALTIVGTLPFTYMLEK.W + 5 Phospho (ST)
442 − 458	12	K.QALTIVGTLPFTYMLEK.W + Phospho (ST); GlyGly (K)
442 − 458	12	K.QALTIVGTLPFTYMLEK.W + Phospho (ST)
535 − 553	3	K.HEGPLHKCDISNSTEAGQK.L + 2 Phospho (ST); 2 GlyGly (K)
542 − 553	11	K.CDISNSTEAGQK.L + Carbamidomethyl (C); GlyGly (K)
542 − 553	6	K.CDISNSTEAGQK.L + Phospho (ST); GlyGly (K)
542 − 553	7	K.CDISNSTEAGQK.L + Phospho (ST); GlyGly (K)
542 − 553	15	K.CDISNSTEAGQK.L + 3 Phospho (ST); GlyGly (K)
542 − 553	16	K.CDISNSTEAGQK.L + Carbamidomethyl (C); Phospho (ST)
542 − 553	16	K.CDISNSTEAGQK.L + Carbamidomethyl (C); Phospho (ST)
560 − 577	18	R.LGKSEPWTLALENVVGAK.N + GlyGly (K); LeuArgGlyGly (K)
563 − 596	16	K.SEPWTLALENVVGAKNMNVRPLLNYFEPLFTWLK.D + 2 Phospho (ST); 2 GlyGly (K)
578 − 596	15	K.NMNVRPLLNYFEPLFTWLK.D + Phospho (ST); LeuArgGlyGly (K)
601 − 621	15	K.NSFVGWSTDWSPYADQSIKVR.I + Phospho (ST); Phospho (Y); LeuArgGlyGly (K)
601 − 621	13	K.NSFVGWSTDWSPYADQSIKVR.I + 4 Phospho (ST)
601 − 625	13	K.NSFVGWSTDWSPYADQSIKVRISLK.S + Phospho (ST); Phospho (Y); 2 GlyGly (K)
620 − 631	8	K.VRISLKSALGDK.A + Phospho (ST); 2 GlyGly (K)
620 − 631	11	K.VRISLKSALGDK.A + 2 Phospho (ST); 2 GlyGly (K)
620 − 631	13	K.VRISLKSALGDK.A + Phospho (ST); GlyGly (K)
620 − 631	3	K.VRISLKSALGDK.A + Phospho (ST); GlyGly (K); LeuArgGlyGly (K)
620 − 631	1	K.VRISLKSALGDK.A + LeuArgGlyGly (K)
622 − 631	10	R.ISLKSALGDK.A + Phospho (ST); 2 GlyGly (K)
622 − 631	12	R.ISLKSALGDK.A + 2 Phospho (ST); 2 GlyGly (K)
622 − 631	13	R.ISLKSALGDK.A + 2 Phospho (ST); GlyGly (K); LeuArgGlyGly (K)
626 − 644	15	K.SALGDKAYEWNDNEMYLFR.S + GlyGly (K)
645 − 657	8	R.SSVAYAMRQYFLK.V + Phospho (ST); GlyGly (K)
690 − 697	5	K.NVSDIIPR.T + Phospho (ST)
690 − 702	3	K.NVSDIIPRTEVEK.A + GlyGly (K)
690 − 702	12	K.NVSDIIPRTEVEK.A + GlyGly (K)
709 − 716	2	R.SRINDAFR.L + Phospho (ST)
709 − 716	3	R.SRINDAFR.L + Phospho (ST)

709 − 716	6	R.SRINDAFR.L + Phospho (ST)
709 − 716	4	R.SRINDAFR.L + Phospho (ST)
772 − 788	16	K.NKARSGENPYASIDISK.G + 2 GlyGly (K)
772 − 788	13	K.NKARSGENPYASIDISK.G + 2 GlyGly (K)
772 − 788	3	K.NKARSGENPYASIDISK.G + GlyGly (K)
774 − 788	22	K.ARSGENPYASIDISK.G + GlyGly (K)
774 − 788	16	K.ARSGENPYASIDISK.G + GlyGly (K)
774 − 788	15	K.ARSGENPYASIDISK.G + GlyGly (K)
774 − 788	13	K.ARSGENPYASIDISK.G + GlyGly (K)
774 − 788	10	K.ARSGENPYASIDISK.G + GlyGly (K)
774 − 788	12	K.ARSGENPYASIDISK.G + GlyGly (K)
774 − 788	10	K.ARSGENPYASIDISK.G + GlyGly (K)
774 − 788	7	K.ARSGENPYASIDISK.G + Phospho (ST); GlyGly (K)
774 − 788	15	K.ARSGENPYASIDISK.G + Phospho (Y); GlyGly (K)
774 − 788	7	K.ARSGENPYASIDISK.G + Phospho (Y); GlyGly (K)
774 − 788	12	K.ARSGENPYASIDISK.G + Phospho (ST); GlyGly (K)
774 − 788	17	K.ARSGENPYASIDISK.G + Phospho (ST); GlyGly (K)
774 − 788	9	K.ARSGENPYASIDISK.G + Phospho (ST); GlyGly (K)
774 − 788	14	K.ARSGENPYASIDISK.G + Phospho (ST); GlyGly (K)
774 − 788	12	K.ARSGENPYASIDISK.G + 2 Phospho (ST); GlyGly (K)
774 − 788	19	K.ARSGENPYASIDISK.G + Phospho (ST); Phospho (Y); GlyGly (K)
774 − 788	15	K.ARSGENPYASIDISK.G + 2 Phospho (ST); GlyGly (K)
774 − 788	21	K.ARSGENPYASIDISK.G + 2 Phospho (ST); GlyGly (K)
774 − 788	17	K.ARSGENPYASIDISK.G + Phospho (ST); LeuArgGlyGly (K)
774 − 788	12	K.ARSGENPYASIDISK.G + Phospho (ST); LeuArgGlyGly (K)
776 − 788	22	R.SGENPYASIDISK.G + GlyGly (K)
776 − 788	12	R.SGENPYASIDISK.G + GlyGly (K)
776 − 788	7	R.SGENPYASIDISK.G + Phospho (ST); GlyGly (K)
776 − 788	9	R.SGENPYASIDISK.G + 2 Phospho (ST); GlyGly (K)
776 − 788	15	R.SGENPYASIDISK.G + Phospho (ST); Phospho (Y)
776 − 788	11	R.SGENPYASIDISK.G + 3 Phospho (ST); Phospho (Y); LeuArgGlyGly (K)